3. Results

3.1. Morphological examination

The T-2 toxin treatment in pregnant rats induced histopathological changes such as apoptosis in the fetal brain. Apoptosis was observed in neuroepithelial cells mainly in the outer layer of the ventricular zone of the telencephalon after the T-2 toxin treatment. Apoptotic bodies ingested by neuroepithelial cells were also observed in the telencephalon (Fig. 1). In addition, apoptotic nuclei were positively stained using the TUNEL method (Fig. 2). The TUNEL index was increased at 1 HAT, peaked at 12 HAT, and then slightly decreased at 24 HAT (Figs. 2B–D and 3). In addition to the telencephalon, apoptosis of neuroepithelial cells was also observed in the diencephalon, mesencephalon, metencephalon and myelencephalon. On the other hand, only a few TUNEL-positive cells were observed in the control animals (Fig. 2A).

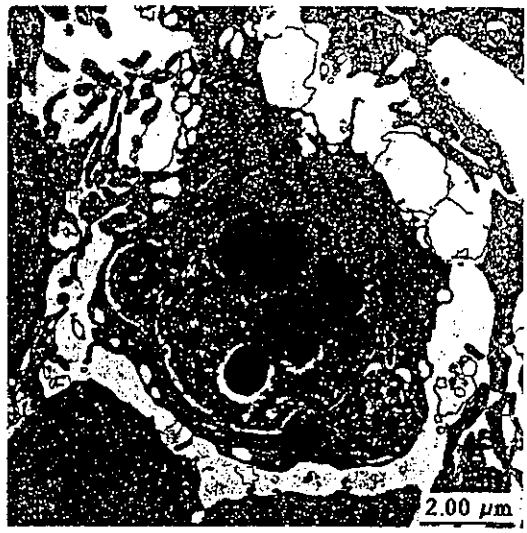

Fig. 1. Electron micrograph of apoptotic bodies ingested by neuroepithelial cells in the telencephalon at 9 HAT.

3.2. Microarray analysis

To investigate gene expression profiles in the fetal brain treated with T-2 toxin, we selected three time points (6, 12 and 24 HAT) for microarray analysis based on the histopathological results. It is known that T-2 toxin induces apoptosis, lipid peroxidation, and suppression of drug-metabolizing enzymes (Chang and Mar, 1988; Guerre et al., 2000; Sehata et al., 2004). Therefore, we focused on the fields of cell growth-, stress-, signal transduction-, and metabolism-related genes in the present study.

Out of 8798 gene probes present on the GeneChip®, the expression of 12 genes (0.14%) was increased and that of 13 genes (0.15%) was decreased at 6 HAT (Table 2). The major classes showing increased expression were genes related to signal transduction (e.g. RAC protein kinase gamma), and those showing decreased expression

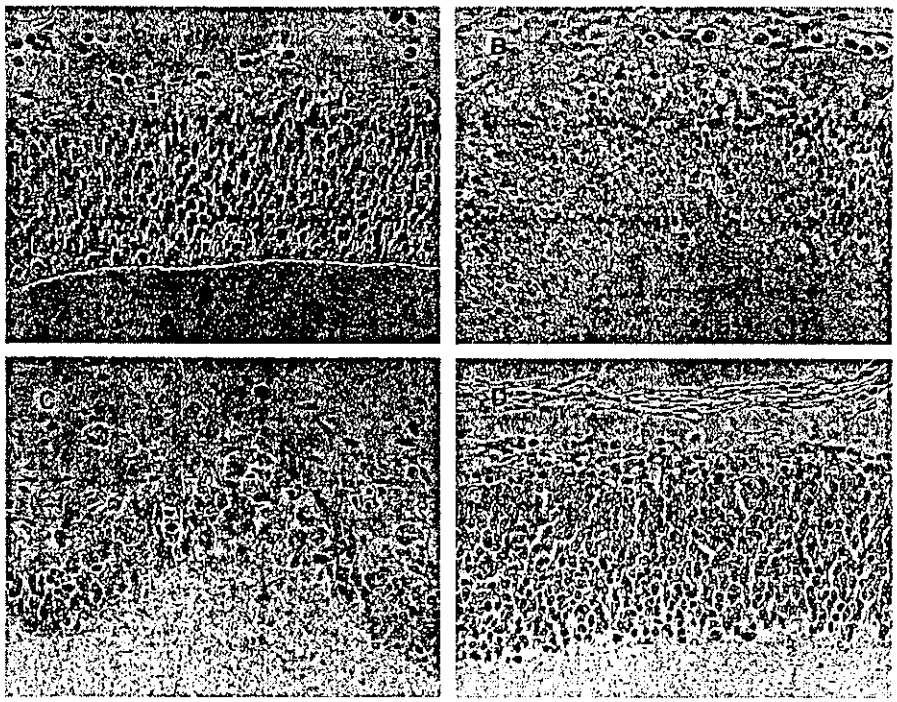

Fig. 2. TUNEL staining in the telencephalon. The number of apoptotic cells in the telencephalic wall was increased by T-2 toxin. Control fetus at 12 HAT (A). T-2 toxin-treated fetus at 6 HAT (B), at 12 HAT (C), and at 24 HAT (D). TUNEL staining, ×250.

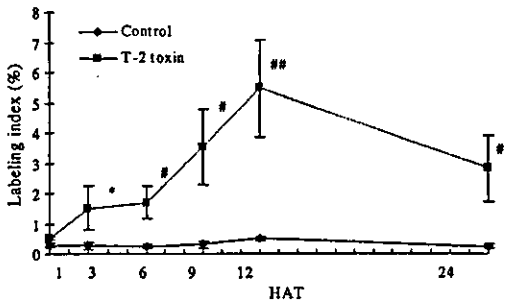

Fig. 3. Changes in the number of TUNEL-positive cells/500 neuroepithelial cells in the telencephalic wall. Each value represents the mean ± SE of 3 fetuses/dam/group. $^{*}p < 0.05$ (Student's t-test), $\#p < 0.05$, $\#\#p < 0.01$ (Welch's t-test).

were metabolism-related genes (e.g. liver stearyl-CoA desaturase).

At 12 HAT, the expression of 44 genes (0.50%) was increased and that of 74 genes (0.84%) was decreased after the T-2 toxin treatment (Table 3). The major classes showing increased expression were genes related to stress (HSP70, metallothionein-2 and -1 and HO-1), cell growth/apoptosis (IGF-BP 3, VEGF-A, c-Ha-ras and TIMP-3) and signal transduction (MEKK1 and IRS-1). The major classes showing decreased expression were genes related to transcription (ania-1), signal transduction (JAK2 and PI3-kinase subunit) and metabolism (liver stearyl-CoA desaturase).

At 24 HAT, the expression of 48 genes (0.55%) was increased and that of 116 genes (1.32%) was decreased after the T-2 toxin treatment (Table 4). The major classes showing increased expression were genes related to cell growth/apoptosis (adrenomedullin precursor, VEGF-3 and RJG-9 gene for c-jun), signal transduction (MEKK1 and caspase-2), and stress (Cu, Zn-SOD). The major classes showing decreased expression were genes related to metabolism (mitochondrial NADH-dehydrogenase, liver stearyl-CoA desaturase, ApoE, fatty acid synthetase and GST Yrs–Yrs), cell growth (PDGF receptor and GAS-7 protein) and signal transduction (INF-gamma receptor and GABA transporter protein).

3.3. Real-time RT-PCR

Based on the results of microarray analysis and histopathological examinations (apoptosis), oxidative stress- and apoptosis-related genes were selected to confirm the changes observed in the microarray analysis. Real-time RT-PCR also showed increased expression of HSP70, HO-1, IGF-BP3 and VEGF-A at 6, 12 and 24 HAT (Table 5).

4. Discussion

T-2 toxin treatment induced apoptosis in the fetal brain in the present study as previously reported in mice and rats (Ishigami et al., 1999, 2001; Sehata et al., 2003). Apoptosis began to be induced from 1 HAT, and peaked at 12 HAT. In rats, it is reported that T-2 toxin passes through the placenta and is distributed to the fetal tissues (Lafarge-Frayssinet et al., 1990). In addition, it is known that the blood brain barrier (BBB) is composed of complex tight junctions (TJ) between the endothelial cells and the overall complexity of the TJ network was increased between embryonic day 18 to postnatal day 1 in rats (Kniesel et al., 1996), suggesting that the BBB was not well developed during embryonic days 13-14 used in the present study. As T-2 toxin and its metabolite HT-2 have a lipophilic nature, it can be speculated that T-2 toxin might be easily distributed to the fetal brain because the fetal brain is rich in lipids. Furthermore, we reported that the apoptosis observed in the fetal tissues was essentially the same as that observed in dams (Sehata et al., 2003). We also reported that oxidative stress-, apoptosis-, lipid metabolism- and drug metabolizing enzyme-related genes were consistently detected in the dam's liver, placenta and fetal liver. In the present study, microarray results in the fetal brain showed similar changes as observed in the reported dam's tissues. Therefore, the changes observed in the fetal brain might be a direct effect of T-2 toxin. To confirm the direct effects of T-2 toxin in the fetal tissues, however, it is necessary to measure the concentration of T-2 toxin in the fetal tissues.

Table 2
Gene expression changes observed in the fetal brain at 6 HAT

Gene	Function	GenBank#	Fold change	t-test
Up-regulated				
cDNA clone rx044573 (similar to transcription initiation factor IID 250K chain splice form 2)	Transcription	AI639315	1.99	0.022
RAC protein kinase gamma	Signal transduction	D49836	1.61	0.026
cDNA clone rx028263 (CED-6 Protein homolog)	Signal transduction	AI639037	1.51	0.020
Down-regulated				
Insulin-induced growth-response protein (CL-6)	Cell growth	L13619	−1.87	0.001
Liver stearyl-CoA desaturase	Metabolism	J02585	−1.73	0.009

Table 3
Gene expression changes observed in the fetal brain at 12 HAT

Gene	Function	GenBank#	Fold change	*t*-test
Up-regulated				
HSP70	Stress	Z27118	145.54	0.040
EST220041 (metallothionein-2 and metallothionein-1)	Stress	AI176456	15.60	0.022
HO	Stress	J02722	6.91	0.015
EST193502 (VEGF-A)	Cell growth	AA850734	2.91	0.037
IGF-BP3	Cell growth	M31837	2.05	0.036
EST194815 (c-Ha-ras proto-oncogene mechanism sequence)	Cell growth	AA852046	1.67	0.032
SHARP-1	Transcription	AF009329	2.65	0.008
Krox-24	Immediate early gene	U75397	2.51	0.049
TIMP-3	Signal transduction	U27201	1.84	0.005
MEKK1	Signal transduction	U48596	1.62	0.025
IRS-1 mRNA for insulin-receptor5	Signal transduction	X58375	1.58	0.017
Type II hexokinase gene	Metabolism	D26393	3.08	0.003
EST195752 (adenylate kinase 4)	Metabolism	AA891949	2.79	0.009
Prolyl 4-hydroxylase alpha subunit	Metabolism	X78949	2.67	0.005
Down-regulated				
PMF16	Transcription	AB006880	−3.16	0.020
BHF-1	Transcription	D82074	−2.08	0.026
Ania-1	Immediate early gene	AF030086	−1.78	0.015
EST196362 (ciliary neurotrophic factor)	Cell growth	AA892559	−2.43	0.009
cDNA clone rx041043 (neurogenic differentiation 1)	Cell growth	AI639109	−2.16	0.026
JAK2	Signal transduction	AJ000557	−1.79	0.011
Phosphatidylinositol 3-kinase p85 beta subunit	Signal transduction	D64046	−1.53	0.018
5-Aminolevulinate synthase	Metabolism	J03190	−2.39	0.004
Liver stearyl-CoA desaturase	Metabolism	J02585	−1.66	0.048

HSP70, heat shock protein 70; HO, hemeoxygenase; VEGF-A, vascular endothelial growth factor A; IGF-BP3, insulin-like growth factor binding protein; SHARP-1, enhancer-of-split and hairy-related protein 1; TIMP-3, tissue inhibitor of metalloproteinase 3; MEKK1, MAP kinase kinase kinase 1; ania-1, activity and neurotransmitter-induced early gene 1; JAK2, Janus protein tyrosine kinase 2.

In this study, to investigate the gene expression profiles induced by T-2 toxin in the fetal brain, a microarray analysis was also performed based on the results of the histopathological examinations. As a result, many genes attributable to the T-2 toxin treatment were detected mainly at 12 HAT. To confirm the changes observed by GeneChip® analysis, we performed real-time RT-PCR on selected genes. Although not all results were completely consistent between GeneChip® analysis and real-time RT-PCR analysis, individual data from both analyses showed good correlation of gene expression changes. Therefore, we concluded that real-time RT-PCR analysis generally confirmed the changes observed by GeneChip® analysis for the representative genes.

It is known that a lack of neurotrophic supports and neurotransmitters, and treatment with neurotoxicants, DNA-damaging chemicals, oxidative stress, nitric oxide and ceramides induce apoptosis in the nervous system (Sastry and Rao, 2000). In the present study, the expression of HSP70, metallothionein (MT)-2 and -1, and HO-1 genes was strongly elevated by T-2 toxin at 12 HAT, and the expression of the Cu,Zn-superoxide dismutase (Cu,Zn-SOD) gene was also increased at 24 HAT. It is reported that oxidative stress and hypoxia may induce the elevation of HSP70, HO, MT and Cu,Zn-SOD gene expression (Ciriolo et al., 2000; Garrido et al., 2001; Hidalgo et al., 2001; Ryter et al., 2002). These findings suggested that the T-2 toxin-induced oxidative stress in the fetal brain. Similar changes in the expression of oxidative stress-related genes were also observed in the dam's liver and placenta and fetal liver in pregnant rats treated with T-2 toxin (Sehata et al., 2004). Therefore, oxidative stress might be the main factor behind the T-2 toxin-induced changes in these tissues.

Mitogen-activated protein kinases (MAPKs) are important factors in signaling pathways involved in cell growth, differentiation and apoptosis. For example, extracellular signal-related protein kinase (ERK) mediates cell growth and protects cells from apoptosis, whereas stress-activated protein kinase (SAPK)/c-Jun N-terminal kinase (JNK) and p38 MAPK inhibit cell proliferation and may promote apoptosis (Jarpe et al., 1998). Each MAPK is activated by an upstream MAPK kinase, including MEKK1, and JNK activates transcription factors such as c-fos and c-jun. MEKK1 may induce apoptosis by causing a general deregulation of MAP kinase signaling (Boldt et al., 2003). It is also reported that JNKs and c-jun are important regulators of apoptosis in the nervous system (Ham et al., 2000). In the present study, the expression of MEKK1 gene was increased at 12 and 24 HAT, and the expression of c-jun gene was increased at 24 HAT. In addition, it

Table 4
Gene expression changes observed in the fetal brain at 24 HAT

Gene	Function	GenBank#	Fold change	*t*-test
Up-regulated				
Adrenomedullin precursor	Cell growth	D15069	7.07	0.035
VEGF3	Cell growth	L20913	2.05	0.022
Immediate early gene transcription factor NGFI-B	Immediate early gene	U17254	2.57	0.002
EST219534 (RJG-9 gene for c-jun)	Transcription	AI175959	1.84	0.049
cDNA (Cbp/p300-interacting transactivator with Glu/Asp-rich carboxy-terminal domain 2)	Transcription	AA900476	1.50	0.020
cAMP phosphodiesterase (PDE4)	Signal transduction	M25350	2.20	0.001
MEKK1	Signal transduction	U48596	1.69	0.042
Caspase 2 (Ich1)	Signal transduction	AF025671	1.62	0.048
Cu,Zn-SOD	Stress	M21060	1.50	0.029
Prolyl 4-hydroxylase alpha subunit	Metabolism	X78949	2.52	0.036
Brain glucose-transporter protein	Transporter	M13979	2.77	0.025
Down-regulated				
NDI	Metabolism	M35826	−5.06	0.038
Mitochondrial cytochrome oxidase subunits I,II, III genes	Metabolism	J01435	−3.48	0.001
Non-hepatic-type S-adenosylmethionine synthetase	Metabolism	AB000717	−3.49	0.004
EST200668 (transthyretin)	Metabolism	AA945169	−3.10	0.009
S-Adenosylmethionine synthetase	Metabolism	J05571	−3.00	0.008
Muscle type calpain p94	Metabolism	AF061726	−2.65	0.005
EST197466 (sialyltransferase 8D)	Metabolism	AA893663	−2.37	0.019
Phospholipase C-beta1b	Metabolism	L14323	−2.04	0.027
GST Yrs–Yrs	Metabolism	D10026	−1.62	0.005
Liver stearyl-CoA desaturase	Metabolism	J02585	−1.59	0.026
Apolipoprotein E (rApoE)	Metabolism	S76779	−1.53	0.032
Fatty acid synthase	Metabolism	M76767	−1.52	0.036
EST194911 (Similar to zinc finger protein 281)	Transcription	AA891108	−3.08	0.004
cDNA (cyclin M4)	Cell growth	AA859983	−2.18	0.013
EST229067 (similar to platelet derived growth factor receptor, alpha polypeptide)	Cell growth	AI232379	−2.14	0.009
EST196362 (ciliary neurotrophic factor)	Cell growth	AA892559	−2.02	0.038
EST198013 (Mit1/Lb9)	Cell growth	AA894210	−2.01	0.028
GAS-7 protein	Cell growth	AJ131902	−1.64	0.025
cDNA (TGFB inducible early growth response)	Immediate early gene	AI071299	−2.14	0.020
EST190205 (ribosomal protein L4)	Translation	AA800708	−2.00	0.015
EST226942 (selenoprotein P)	Stress	AI230247	−2.49	0.016
Lipocortin V	Signal transduction	AF051895	−2.39	0.004
cDNA clone rx050073 (decorin)	Signal transduction	AI639233	−2.40	0.043
cDNA clone rx018443 (RAB33B)	Signal transduction	AI639102	−2.15	0.003
Interferon gamma receptor	Signal transduction	U68272	−1.94	0.040
EST225364 (GABA transporter protein)	Signal transduction	AI228669	−1.70	0.041
CPP32	Signal transduction	U84410	−1.51	0.038
Ras-related mRNA rab3	Signal transduction	X06889	−1.51	0.036
RAC protein kinase beta	Signal transduction	D30041	−1.52	0.010

Cu,Zn-SOD, copper–zinc containing superoxide dismutase; NDI, mitochondrial NADH-dehydrogenase; GST Yrs–Yrs, glutathione S-transferase Yrs–Yrs; CPP32, interleukin-1beta-converting enzyme-related protease.

Table 5
Average fold changes of GeneChip® and real-time RT-PCR analyses

Gene	Hours after treatment					
	6		12		24	
	GeneChip®	RT-PCR	GeneChip®	RT-PCR	GeneChip®	RT-PCR
HSP70	22.55 ± 9.27	13.73 ± 5.89	145.54 ± 29.71#	54.01 ± 20.36	238.97 ± 161.45	287.64 ± 241.30
HO-1	3.06 ± 0.88*	1.60 ± 0.53	6.91 ± 1.44**	1.82 ± 0.68	6.06 ± 1.86	6.57 ± 2.96
IGF-BP3	1.01 ± 0.10	1.08 ± 0.01	2.05 ± 0.33*	1.88 ± 0.37	2.27 ± 0.48	1.70 ± 0.25*
VEGF-A	1.15 ± 0.03	0.93 ± 0.09	2.40 ± 0.41#	2.73 ± 0.08**	2.05 ± 0.27*	3.44 ± 1.22

Mean ± SE. Significant difference from control: $*p < 0.05$, $**p < 0.01$ (Student's *t*-test); $\#p < 0.05$ (Welch's *t*-test).

is reported that T-2 toxin and other trichothecene mycotoxins induce apoptosis by activating MAPKs (Shifrin and Anderson, 1999; Yang et al., 2000). Increased expression of c-fos and c-jun genes in the skin treated with T-2 toxin was reported (Albarenque et al., 2001a). Therefore, our results also suggest that the MAPK-JNK-c-Jun pathway might be involved in T-2 toxin-induced apoptosis in the fetal brain.

Caspase activation is known to play an important role in the induction of apoptosis (Cohen, 1997). It is reported that T-2 toxin induces apoptosis in lymphoid cell lines by activation of caspases (-9 and -3) (Nagase et al., 2001). In the present study, although no changes in the gene expression of caspase-3 or -9 were detected, increased gene expression of caspase-2 was detected at 24 HAT. Activation of caspase-2 is induced by reactive oxygen species and caspase-2 plays critical and singular roles in the control of apoptosis (Annunziato et al., 2003; Troy and Shelanski, 2003). Therefore, the increased gene expression of caspase-2 in the present study may also indicate the involvement of caspase-2 in T-2 toxin-induced apoptosis in the fetal brain.

Tissue inhibitors of metalloproteinase (TIMP)-3 induce a type II apoptotic pathway initiated via a Fas-associated death domain-dependent mechanism with activation of caspase-8 and -9 (Bond et al., 2002). It is known that Fas and TNF-α receptors have a death domain. It is reported that TNF-α mRNA expression might play an important role in T-2 toxin-induced epidermal cell apoptosis (Albarenque et al., 2001b). On the other hand, T-2 toxin-induced apoptosis in thymocytes is independent of the Fas/Fas ligand pathway (Alam et al., 2000). In the present study, although the expression of caspase-8 and -9 was not changed, the expression of the TIMP-3 gene was increased at 12 HAT. Therefore, there is a possibility that the TNF receptor pathway may also be involved in the mechanisms of T-2 toxin-induced apoptosis in the rat fetal brain.

Increased expression of the insulin-like growth factor binding protein-3 (IGF-BP3) gene was observed at 12 HAT. It is known that IGF-BP blocks the effects of IGF and regulates cell growth. The IGF-BP3 gene is a p53-regulated target gene (Buckbinder et al., 1995), and it is well known that p53 plays an important role in apoptosis induction. On the other hand, it is also reported that IGF-BP3 induces apoptosis through a p53 or IGF-receptor-independent pathway (Rajah et al., 1997). Recently, it has been suggested that 9-*cis* retinoic acid receptor-α (retinoid X receptor α, RXRα) is required for IGF-BP3-induced apoptosis (Lee and Cohen, 2002). As the detailed signaling pathway through IGF-BP3 is not yet clear, the role of IGF-BP3 in T-2 toxin-induced apoptosis is still controversial.

At 12 and 24 HAT, the expression of vascular endothelial growth factor (VEGF) gene was increased by the T-2 toxin treatment in the fetal brain. Recently, it has been reported that VEGF is expressed in neurons and may play a role in the maintenance of neurons and endothelial cells in the central nervous system (Ogunshola et al., 2002). In addition, it is also reported that VEGF and its receptor might be important for neuronal survival (Jin et al., 2000; Ogunshola et al., 2002). Therefore, the observed VEGF induction in the present study might indicate a protective reaction to the apoptotic changes in the fetal brain induced by T-2 toxin.

There were many metabolism-related genes that showed a decreased expression at 12 and 24 HAT. The gene expression of liver stearyl-CoA desaturase and farnesyl diphosphate synthase genes was suppressed by T-2 toxin both at 12 and 24 HAT. These genes are involved in lipid metabolism. T-2 toxin causes lipid peroxidation in the membrane system (Chang and Mar, 1988), and, therefore, this result might reflect T-2 toxin-induced effects on lipid metabolism. The suppression of drug metabolizing enzymes (GSTs in the present study) by T-2 toxin is consistent with the results of reported experiments (Galtier et al., 1989; Guerre et al., 2000). In addition, a decreased expression in mitochondria-related genes, such as mitochondrial NADH-dehydrogenase and cytochrome oxidase, and mitochondria genome, was observed at 24 HAT, suggesting a dysfunction of the mitochondria as a result of the T-2 toxin treatment. Since mitochondria play an important role in cell survival, these changes in metabolism-related genes may also have a relationship to the induction of apoptosis.

Taken together, T-2 toxin-induced apoptosis in neuroepithelial cells in the fetal rat brain. Microarray analysis showed that the expression of oxidative stress-related genes was strongly induced by T-2 toxin at 12 HAT, i.e. the peak time point of apoptosis induction. The expression of apoptosis-related genes (MEKK1, c-jun, IGF-BP3 and TIMP-3) was also induced after the T-2 toxin treatment. Our results suggest that T-2 toxin-induced apoptosis in the fetal rat brain may be due to the induction of oxidative stress following the activation of the MAPK pathway. However, there is also a possibility that the TNF receptor- or IGF-BP3-related pathway may be involved in T-2 toxin-induced apoptosis. Further studies are needed to investigate the detailed mechanisms involved in T-2 toxin-induced toxicity.

Acknowledgments

We thank Mrs. K. Hara and Mrs. K. Ishikawa for the preparation of pathological samples and Miss K. Sakuma and Mrs. N. Niino for conducting the microarray and real-time RT-PCR analyses.

References

Alam, M.M., Nagase, M., Yoshizawa, T., Sakato, N., 2000. Thymocyte apoptosis by T-2 toxin in vitro in mice is independent of Fas/Fas ligand system. Bioscience, Biotechnology, and Biochemistry 64, 210–213.

Albarenque, S.M., Suzuki, K., Shinozuka, J., Nakayama, H., Doi, K., 2001a. Kinetics of apoptosis-related genes mRNA expression in the dorsal skin of hypotrichotic WBN/ILA-*Ht* rats after topical application of T-2 toxin. Experimental and Toxicologic Pathology 52, 553–556.

Albarenque, S.M., Suzuki, K., Nakayama, H., Doi, K., 2001b. Kinetics of cytokines mRNAs expression in the dorsal skin of WBN/ILA-*Ht* rats following topical application of T-2 toxin. Experimental and Toxicologic Pathology 53, 271–274.

Annunziato, L., Amoroso, S., Pannaccione, A., Cataldi, M., Pignataro, G., D'Alessio, A., Sirabella, R., Secondo, A., Sibaud, L., Di Renzo, G.F., 2003. Apoptosis induced in neuronal cells by oxidative stress: role played by caspases and intracellular calcium ions. Toxicology Letters 139, 125–133.

Boldt, S., Weidle, U.H., Kolch, W., 2003. The kinase domain of MEKK1 induces apoptosis by dysregulation of MAP kinase pathways. Experimental Cell Research 283, 80–90.

Bond, M., Murphy, G., Bennett, M.R., Newby, A.C., Baker, A.H., 2002. Tissue inhibitor of metalloproteinase-3 induces a Fas-associated death domain-dependent type II apoptotic pathway. The Journal of Biological Chemistry 277, 13787–13795.

Buckbinder, L., Talbott, R., Velasco-Miguel, S., Takenaka, I., Faha, B.R., Seizinger, B.R., Kley, N., 1995. Induction of the growth inhibitor IGF-binding protein 3 by p53. Nature 377, 646–649.

Bulera, S.J., Eddy, S.M., Ferguson, E., Jatkoe, T.A., Reindel, J.F., Bleavins, M.R., De La Iglesia, F.A., 2001. RNA expression in the early characterization of hepatotoxicants in Wistar rats by high-density DNA microarrays. Hepatology 33, 1239–1258.

Chang, I.-M., Mar, W.-C., 1988. Effect of T-2 toxin on lipid peroxidation in rats: elevation of conjugated diene formation. Toxicology Letters 40, 275–280.

Ciriolo, M.R., De Martino, A., Lagavia, E., Rossi, L., Carri, M.T., Rotilio, G., 2000. Cu,Zn-superoxide dismutase-dependent apoptosis induced by nitric oxide in neuronal cells. The Journal of Biological Chemistry 275, 5065–5072.

Cohen, G.M., 1997. Caspases: the executioners of apoptosis. Biochemical Journal 326, 1–16.

Galtier, P., Paulin, F., Eeckhoutte, C., Larrieu, G., 1989. Comparative effects of T-2 toxin and diacetoxyscirpenol on drug metabolizing enzymes in rat tissues. Food and Chemical Toxicology 27, 215–220.

Garrido, C., Gurbuxani, S., Ravagnan, L., Kroemer, G., 2001. Heat shock proteins: endogenous modulators of apoptotic cell death. Biochemical and Biophysical Research Communications 286, 433–442.

Guerre, P., Eeckhoutte, C., Burgat, V., Galtier, P., 2000. The effects of T-2 toxin exposure on liver drug metabolizing enzymes in rabbit. Food Additives and Contaminants 17, 1019–1026.

Ham, J., Eilers, A., Whitfield, J., Neame, S.J., Shah, B., 2000. c-Jun and the transcriptional control of neuronal apoptosis. Biochemical Pharmacology 60, 1015–1021.

Hayes, M.A., Schiefer, F.B., 1982. Comparative toxicity of dietary T-2 toxin in rats and mice. Journal of Applied Toxicology 2, 207–211.

Hidalgo, J., Aschner, M., Zatta, P., Vasak, M., 2001. Roles of the metallothionein family of proteins in the central nervous system. Brain Research Bulletin 55, 133–145.

Hoerr, F.J., Carlton, W.W., Yagen, B., 1981. Mycotoxicosis caused by a single dose of T-2 toxin or diacetoxyscirpenol in broiler chickens. Veterinary Pathology 18, 652–664.

Ishigami, N., Shinozuka, J., Katayama, K., Uetsuka, K., Nakayama, K., Doi, K., 1999. Apoptosis in the developing mouse embryos from T-2 toxin-inoculated dams. Histology and Histopathology 14, 729–733.

Ishigami, N., Shinozuka, J., Katayama, K., Uetsuka, K., Nakayama, K., Doi, K., 2001. Apoptosis in mouse fetuses from dams exposed to T-2 toxin at different days of gestation. Experimental and Toxicologic Pathology 52, 493–501.

Jarpe, M.B., Widmann, C., Knall, C., Schlesinger, T.K., Gibson, S., Yujiri, T., Fanger, G.R., Gelfand, E.W., Johnson, G.L., 1998. Anti-apoptotic versus pro-apoptotic signal transduction: checkpoints and stop signs along the road to death. Oncogene 17, 1475–1482.

Jin, K.L., Mao, X.O., Greedberg, D.A., 2000. Vascular endothelial growth factor: direct neuroprotective effect in vitro ischemia. Proceedings of the National Academy of Sciences 97, 10242–10247.

Kniesel, U., Risau, W., Wolburg, H., 1996. Development of blood-brain barrier tight junctions in the rat cortex. Brain Research. Developmental Brain Research 23, 229–240.

Lafarge-Frayssinet, C., Chakor, K., Lafont, P., Frayssinet, C., 1990. Transplacentral transfer of T2-toxin: pathological effect. Journal of Environmental Pathology, Toxicology and Oncology 10, 64–68.

Lee, K.-W., Cohen, P., 2002. Nuclear effects: unexpected intracellular actions of insulin-like growth factor binding protein-3. Journal of Endocrinology 175, 33–40.

Marasas, W.F.O., Bamburg, J.R., Smalley, E.B., Strong, F.M., Ragland, W.L., Degurse, P.E., 1969. Toxic effects on trout, rats, and mice of T-2 toxin produced by the fungus *Fusarium tricinctum* (Cd.) Snyd. Et Hans. Toxicology and Applied Pharmacology 15, 471–482.

Martin, L.J., Morse, J.D., Anthony, A., 1986. Quantitaive cytophotometric analysis of brain neuronal RNA and protein changes in acute T-2 mycotoxin poisoned rats. Toxicon 24, 933–941.

Middlebrook, J.L., Leatherman, D.L., 1989. Binding of T-2 toxin to eukaryotic cell ribosomes. Biochemical Pharmacology 38, 3103–3110.

Nagase, M., Alam, M.M., Tsushima, A., Yoshizawa, T., Sakato, N., 2001. Apoptosis induction by T-2 toxin: activation of caspase-9, caspase-3, and DFF-40/CAD through cytosolic release of cytochrome c in HL-60 cells. Bioscience, Biotechnology, and Biochemistry 65, 1741–1747.

Ogunshola, O.O., Antic, A., Donoghue, M.J., Fan, S.-Y., Kim, H., Stewart, W.B., Madri, J.A., Ment, L.R., 2002. Paracrine and autocrine function of neuronal vascular endothelial growth factor (VEGF) in the central nervous system. The Journal of Biological Chemistry 277, 11410–11415.

Pang, V.F., Lorenzana, R.M., Beasley, V.R., Buck, W.B., Haschek, W.M., 1987. Experimental T-2 toxicosis in swine: III. Morphologic changes following intravascular administration of T-2 toxin. Fundamental and Applied Toxicology 8, 298–309.

Rajah, R., Valentinis, B., Cohen, P., 1997. Insulin-like growth factor (IGF)-binding protein-3 induces apoptosis and mediates the effects of transforming growth factor-β 1 on programmed cell death through a p53- and IGF-independent mechanism. The Journal of Biological Chemistry 272, 12181–12188.

Rousseaux, C.G., Schiefer, H.B., 1987. Maternal toxicity, embryolethality and abnormal fetal development in CD-1 mice following one oral dose of T-2 toxin. Journal of Applied Toxicology 7, 281–288.

Ryter, S.W., Otterbein, L.E., Morse, D., Choi, A.M., 2002. Heme oxygenase/carbon monoxide signaling pathways: regulation and functional significance. Molecular and Cellular Biochemistry 234–235, 249–263.

Sastry, P.S., Rao, K.S., 2000. Apoptosis and the nervous system. Journal of Neurochemistry 74, 1–20.

Sehata, S., Teranishi, M., Atsumi, F., Uetsuka, K., Nakayama, H., Doi, K., 2003. T-2 toxin-induced morphological changes in pregnant rats. Journal of Toxicologic Pathology 16, 59–65.

Sehata, S., Kiyosawa, N., Sakuma, K., Ito, K., Yamoto, T., Teranishi, K., Uetsuka, K., Nakayama, H., Doi, K., 2004. Gene expression profiles in pregnant rats treated with T-2 Toxin. Experimental and Toxicologic Pathology 55, 357–366.

Shifrin, V.I., Anderson, P., 1999. Trichothecene mycotoxins trigger a ribotoxic stress response that activates c-Jun N-terminal kinase and p38 mitogen-activated protein kinase and induces apoptosis. The Journal of Biological Chemistry 274, 13985–13992.

Shinozuka, J., Suzuki, M., Noguchi, N., Sugimoto, T., Uetsuka, K., Nakayama, H., Doi, K., 1998. T-2 toxin-induced apoptosis in hematopoietic tissues of mice. Toxicologic Pathology 26, 674–681.

Stanford, G.K., Hood, R.D., Hayes, A.W., 1975. Effect of prenatal administration of T-2 toxin to mice. Research Communications in Chemical Pathology and Pharmacology 10, 743–746.

Sugamata, M., Hattori, T., Ihara, T., Okumura, H., Yoshino, N., Ueno, Y., 1998. Fine structural changes and apoptotic cell death by T-2 mycotoxin. The Journal of Toxicological Sciences 23 (Suppl. II), 148–154.

Thompson, W.L., Wannemacher Jr., R.W., 1990. In vivo effects of T-2 mycotoxin on synthesis of proteins and DNA in rat tissues. Toxicology and Applied Pharmacology 105, 483–491.

Troy, C.M., Shelanski, M.L., 2003. Caspase-2 redux. Cell Death and Differentiation 10, 101–107.

Wang, J., Fitzpatrick, D.W., Wilson, J.R., 1998a. Effects of the trichothecene mycotoxin T-2 toxin on neurotransmitters and metabolites in discrete areas of the rat brain. Food and Chemical Toxicology 36, 947–953.

Wang, J., Fitzpatrick, D.W., Wilson, J.R., 1998b. Effect of T-2 toxin on blood-brain barrier permeability monoamine oxidase activity and protein synthesis in rats. Food and Chemical Toxicology 36, 955–961.

Waring, J.F., Jolly, R.A., Ciurlionis, R., Lum, P.Y., Praestgaard, J.T., Morfitt, D.C., Buratto, B., Roberts, C., Schadt, E., Ulrich, R.G., 2001. Clustering of hepatotoxins based on mechanism of toxicity using gene expression profiles. Toxicology and Applied Pharmacology 175, 28–42.

WHO (World Health Organization), 1990. Selected mycotoxins: ochratoxins, trichothecenes, ergot. In: Environmental Health Criteria 105, WHO, Geneva.

Yang, G.-H., Jarvis, B.B., Chung, Y.-J., Pestka, J.J., 2000. Apoptosis induction by the satratoxins and other trichothecene mycotoxins: relationship to ERK, p38 MAPK, and SAPK/JNK activation. Toxicology and Applied Pharmacology 164, 149–160.

Yang, M.C.K., Ruan, Q.G., Yang, J.J., Eckenrode, S., Wu, S., McIndoe, R.A., She, J.X., 2001. A statistical method for flagging weak spots improves normalization and ratio estimates in microarrays. Physiological Genomics 7, 45–53.

Exp Toxic Pathol 2004; 55: 357–366
http://www.elsevier-deutschland.de/etp

[1]Department of Veterinary Pathology, Graduate School of Agricultural and Life Sciences, The University of Tokyo, Bunkyo-ku, Tokyo, Japan
[2]Medicinal Safety Research Laboratories, Sankyo Co., Ltd., Fukuroi-shi, Shizuoka, Japan

Gene expression profiles in pregnant rats treated with T-2 toxin

SHINYA SEHATA[1,2], NAOKI KIYOSAWA[2], KYOKO SAKUMA[2], KAZUMI ITO[2], TAKASHI YAMOTO[2], MUNEHIRO TERANISHI[2], KOJI UETSUKA[2], HIROYUKI NAKAYAMA[2], and KUNIO DOI[2]

With 3 figures and 5 tables

Received: September 11, 2003; Revised: November 03, 2003; Accepted: November 21, 2003

Address for correspondence: SHINYA SEHATA, Department of Veterinary Pathology, Graduate School of Agricultural and Life Sciences, The University of Tokyo, 1-1-1 Yayoi, Bunkyo-ku, Tokyo 113-8657, Japan; Fax: ++81-3-5841-8185; e-mail: asehata@mail.ecc.u-tokyo.ac.jp or sehata@fuku.sankyo.co.jp

Key words: T-2 toxin; pregnant rats; liver; placenta; fetal liver; microarray.

Summary

Pregnant rats on day 13 of gestation were treated orally with T-2 toxin at a single dose of 2 mg/kg and sacrificed at 24 hours after treatment. Histopathologically, apoptosis was increased in the liver, placenta and fetal liver. Microarray analysis was performed to examine the gene expression in the liver, placenta, and fetal liver. The results of microarray analysis showed that the changes in the expression of apoptosis genes, metabolic enzymes and oxidative stress-related genes were detected in these tissues. Suppression of phase I and II enzymes-related genes expression in the liver, and suppression of phase II enzymes-related genes expression in the placenta and fetal liver were observed. Semiquantitive RT-PCR analysis also showed the same results as those of microarray analysis. From the results of microarray analysis and histopathological examination, T-2 toxin seems to induce oxidative stress in these tissues, following the changes in metabolism-related genes expression. These changes may alter the intracellular environments resulting in the induction of apoptosis. Further studies on the gene expression profiles at the earlier time point are necessary to clarify the detailed mechanisms of T-2 toxin-induced toxicity in pregnant rats.

Introduction

T-2 toxin is a trichothecene mycotoxin produced by various species of *Fusarium* spp. *Fusarium* spp. may occur in cereals including corn, oats, rice, and wheat. T-2 toxin has been found to contaminate foods, animal foods and agricultural products, and has been reported in many parts of the world (IARC 1993; WHO 1990). Single dose or subacute dose of T-2 toxin induces damage in the lymphoid and hematopoietic tissues, resulting in lymphopenia and immunosuppression in many species including chickens, mice, rats, rabbits and pigs. Necrosis/apoptosis is also reported in the gastrointestinal tract and liver (BRATICH et al. 1990; HAYES et al. 1982; HOERR et al. 1981; KOSURI et al. 1971; MARASAS et al. 1969; PANG et al. 1987). Furthermore, it is said that pregnant mice treated with T-2 toxin exhibited fetal death and fetotoxicity mainly in the central nervous and skeletal systems in addition to maternal toxicity (ISHIGAMI et al. 2001; ROUSSEAUX et al. 1987; STANFORD et al. 1975). In rats, it is reported that T-2 toxin passes the placenta and distributes to fetal tissues, resulting in an impairment of the immune system (LAFARGE-FRAYSSINET et al. 1990). We have shown that single cell necrosis was observed in the thymus, liver, intestines, placenta and fetal liver in pregnant rats treated with T-2 toxin on day 13 of gestation (SEHATA et al. 2003). However, mechanisms of fetotoxicity induced by T-2 toxin are still unknown.

Recent years DNA microarray technologies have been developed that allow one to detect the expression of many genes at the same time. The application of this technology to the field of toxicology, i.e. toxicogenomics, has been demonstrated. The expression of genes was reported in rats administered with hepatotoxicants, phenobarbital and carbon tetrachloride (BULERA et al. 2001; WARING et al. 2001). There is only one report of microarray analysis in mycotoxin-induced toxicity in animals (LUEHE et al. 2003). They reported that ochratoxin A-

0940-2993/04/55/05-357 $ 15.00/0

specific transcriptional changes were detected for genes involved in DNA damage response and apoptosis, response to oxidative stress, and inflammatory reactions. The purpose of the present study was to examine the gene expression profiles in the liver, placenta, and fetal liver in pregnant rats treated with T-2 toxin. We especially focused on genes related to apoptosis, metabolism, and oxidative stress as major mechanisms involved in the T-2 toxin-induced toxicity. The protocol of this study was approved by the Animal Care and Use Committee of Graduated School of Agricultural and Life Sciences, The University of Tokyo.

Materials and methods

Animals: Six pregnant Wistar: Slc rats (Japan SLC Co., Ltd., Hamamatsu, Japan) on day 11 of gestation (GD11) were obtained from Japan SLC Co., Ltd., Hamamatsu, Japan. Animals were kept using an isolator caging system (Niki Shoji Co., Ltd., Tokyo, Japan) under controlled conditions (23 ± 2 °C with 55 ± 5% humidity and a 14-hr light/10-hr dark cycle), and fed commercial pellets (MF; Oriental Yeast Co., Ltd., Tokyo, Japan) and water *ad libitum*.

Treatment: According to the results from dose-finding study (data not shown) and reported study (SEHATA et al. 2003), animals were used on GD13. Three animals were treated with a single oral dose of 2 mg/kg T-2 toxin (Sigma Chemical Co., St. Louis, MO, USA), and animals were sacrificed by exsanguination under ether anesthesia at 24 hours after treatment (HAT). T-2 toxin was dissolved in corn oil and a dosing volume was adjusted to 2.5 mL/kg. In addition, 3 control animals were treated with the vehicle, and were sacrificed in the same way at 24 HAT.

Histopathological examination and immunohistochemical staining: After animals were sacrificed, macroscopic examination was performed. Dam's organs (liver and thymus) and fetuses were weighed. Dam's organs, and 3 placentae and fetuses from each dam were fixed in 10% neutral-buffered formalin to confirm the changes induced by the T-2 toxin. Four-μm paraffin sections were stained with hematoxylin and eosin (HE) and subjected to microscopic examination. Cells with fragmented DNA were detected by the TdT mediated dUTP nick end labeling (TUNEL) method using an apoptosis detection kit (Apop Tag, Intergen, Purchase, NY, USA). In brief, multiple fragmented DNA-3'-OH ends on the section were labeled with digoxigenin-dUTP in the presence of terminal deoxynucleotidyl transferase (TdT). Peroxidase-conjugated anti-digoxigenin antibody was then reacted with the sections. Apoptotic nuclei were visualized by peroxidase-diaminobenzidine (DAB) reaction. The sections were then counterstained with methyl green. Morphometry was performed in the liver, placenta (3 placentae/dam) and fetal liver (3 fetuses/dam) under light microscope (×400). The number of positive cells/1000 cells was represented as the mean ± SD. Statistical analysis was carried out by Student's *t*-test or Welch's *t*-test after analysis of homogeneity of variance by F-test.

RNA extraction and microarray analysis: Total RNA was extracted from frozen tissues (up to 0.5 g) using the RNeasy Mini Kit (QIAGEN Inc., CA, USA) for the fetal liver or TRIzol reagent (Invitrogen, CA, USA) for the liver and placenta. The RNA from placenta and fetal liver from each dam were pooled to generate a single sample, respectively. Microarray analysis (total 18 arrays) was performed according to the Affymetrix protocol. Briefly, cDNA was prepared from 5 μg of total RNA using the SuperScript Choice System for cDNA Synthesis (Invitrogen, CA, USA), with the exception that primer used for the reverse transcription reaction was T7-(dT)24 primer (Primer sequence: 5'-GGCCAGTGAATTGTAATACGACTCACTAT AGGGAGGCGG-$(dT)_{24}$-3', Amersham Bioscience, Tokyo, Japan). Following this, biotin-labeled cRNA was synthesized from the cDNA using the Enzo High Yield RNA Transcription Labeling Kit (Enzo Diagnostics, NY, USA). After 20 μg biotin-labeled cRNA was fragmentated, hybridization solution was prepared using GeneChip® Eukaryotic Hybridization Control Kit (Affymetrix), and was hybridized to the Affymetrix Rat Genome U34A oligonucleotide array for 45 °C, 16 hours in GeneChip® Hybridization Oven 640 (Affymetrix). The chips were washed and stained using the Fluidics Station (Affymetrix Inc.) and scanned with GeneArray® Scanner (Hewlett-Packard, Palo Alto, CA, USA).

Data analysis: The microarray imaging data were analyzed using the Microarray Suite ver. 5.0 (Affymetrix) and Spotfire Pro Version 4.2 program (Spotfire Inc., MA, USA). In brief, total array normalization (global normalization after trimming the top 2% and bottom 2% of the data) was performed in each experimental data (YANG et al. 2001). Following this, data were compared between the treated group and control group by calculating the prediction value in neighborhood analysis (designed as *Distinction value* in this study, given by (Average A-Average B/(Standard deviation A+ Standard deviation B, Group A and B, GOLUB et al. 1999). In the present study, we only analyzed known genes. Therefore, unknown genes, such as EST genes, were removed from the data. In addition, probes containing at least one Absence Call in the data were also removed. Finally, we selected genes that gave a distinction value of greater than +1.5 or less than −1.5. The mean value of each gene in the treated group was compared with that of control group by Student's *t*-test or Welch's *t*-test after analysis of homogeneity of variance by F-test. A significance level of $p < 0.01$ or $p < 0.05$ was considered acceptable.

Semiquantitive reverse transcriptase polymerase chain reaction (RT-PCR): Total RNA was prepared as described above. The first strand cDNA was synthesized using oligo $(dT)_{12-18}$ primer and the Superscript II RNase H^- Reverse transcriptase (Invitrogen, CA, USA). PCR was performed using oligonucleotide primers sets corresponding to the cDNA sequences (table 1; CYP1A1, CYP2B1/2, CYP2E1, CYP3A1, CYP4A1, GSTA1, GSTA2, GST-P, p53, p21, GADD45, c-fos, c-jun, Bax, hemeoxygenase-1, thioredoxin reductase, heat shock protein 70, and GAPDH) (ALBARENQUE et al. 2001; GAN et al. 2002; KATAYAMA et al. 2002; LIU et al. 2001; LUCERI et al. 2002; MORRIS and DAVILA 1996; NAKAHARA et al. 2002; UENO et al. 2002;

VANHAECKE et al. 2000). As we focused on metabolism, apoptosis, and oxidative stress as major mechanisms involved in T-2 toxin-induced toxicity, we selected the above-mentioned genes. Briefly, 100 μL reaction mixture containing 10 μL 10 × PCR buffer (100 mM Tris-HCl buffer, 500 mM KCl, and 15 mM $MgCl_2$; Takara, Shiga, Japan), 10 μL dNTP (Takara), 50 pmol sense and antisense primer, and 1 μL cDNA sample. PCR reaction (× each cycle numbers (table 1); denaturation at 95 °C for 1 min, annealing at 58 °C for 1 min, and extension at 72 °C for 1 min) was performed using Takara PCR Thermal cycler SP (Takara). The PCR products were electrophoresed in 2% Agarose S (Nippon Gene, Japan)/1 × TBE buffer (89 mM Tris aminomethane, 89 mM Boric acid, 10 mM EDTA). The gels were stained with ethidium bromide (Invitrogen). Fluorescent band was visualized using a UV-CCD video system ($EpiLight_{UVFA1100}$; AISIN COSMOS, Tokyo, Japan) and was analyzed using an image-analysis software, Quantity One (pdi, NY, USA) on a computer. Relative band intensity against GAPDH band was represented as the mean ± standard deviation (SD) of 3 samples. Statistical analysis for the mean values was carried out by F-test followed with Student's *t*-test or Welch's *t*-test.

Results

Histopathological examination

Dam's liver weight was significantly decreased by T-2 toxin. Although thymus weight and fetal weight were not significantly changed, the weights showed a tendency to be decreased (data not shown). At 24 HAT, apoptosis of hepatocytes, cell infiltration and fatty change were observed in the liver from pregnant rats treated with T-2 toxin (fig. 1A). In the placenta, hemorrhage and apoptosis

Table 1. Primer sequences and cycle numbers.

Gene		Sequence	Cycle number			Annealing temperature
			Liver	Placenta	Fetal liver	
CYP1A1	Sense	CTGGTTCTGGATACCCAGCTG	33	31	33	60 °C
	Antisense	CCTAGGGTTGGTTACCAGG				
CYP2B1/2	Sense	GAGTTCTTCTCTGGGTTCCTG	25	28	30	56 °C
	Antisense	ACTGTGGGTCATGGAGAGCTG				
CYP2E1	Sense	CTCCTCGTCATATCCATCTG	20	32	31	56 °C
	Antisense	GCAGCCAATCAGAAATGTGG				
CYP3A1	Sense	ATCCGATATGGAGATCAC	21	35	29	54 °C
	Antisense	GAAGAAGTCCTTGTCTGC				
CYP4A1	Sense	GGTGACAAAGAACTACAGC	24	32	30	54 °C
	Antisense	AGAGGAGTCTTGACCTGCCAG				
GST A1(Ya)	Sense	ATGAGAAGTTTATACAAAGTCC	24	30	35	54 °C
	Antisense	GATCTAAAATGCCTTCGGTG				
GST A2(Yc)	Sense	GATTGACATGTATTCAGAGGGT	23	28	29	56 °C
	Antisense	TTTGCATCCATGGCTGGCTT				
GST-P	Sense	TGCCACCGTACACCATTGTGT	26	23	23	60 °C
	Antisense	CAGCAGGTCCAGCAAGTTGTA				
p53	Sense	ATATGAGCATCGAGCTCCCTCT	34	34	30	58 °C
	Antisense	CACAACTGCACAGGGCATGT				
p21	Sense	AAGTATGCCGTCGTCTGTTCG	29	27	29	58 °C
	Antisense	GGCACTTCAGGGCTTTCTCTT				
GADD45	Sense	GATCGAAAGGATGGACACGG	28	27	28	58 °C
	Antisense	CCCACTGATCCATGTAGCGA				
c-fos	Sense	CATGGACGCTGAAGAGCTACA	34	30	32	58 °C
	Antisense	ACTGACTGAGCTGGTGCATTAC				
c-jun	Sense	CCTACGGCTACAGTAACCCTAA	30	27	27	58 °C
	Antisense	CAGCGTATTCTGGCTATGCAGTT				
Bax	Sense	TTCATCCAGGATCGAGCAGAG	28	26	25	58 °C
	Antisense	TGAGGACTCCAGCCACAAAGAT				
Heme oxygenase-1	Sense	AGCATGCCCCAGGATTTG	30	30	30	58 °C
	Antisense	CTAGCTGGATGTTGAGCAGGA				
Thioredoxin reductase	Sense	GGGAAATTCATTGGTCCTCA	27	26	25	58 °C
	Antisense	CACAGCAGCCATACTCCAAA				
Heat shock protein 70	Sense	GAGTCCTACGCCTTCAATATGAAG	35	31	35	58 °C
	Antisense	CATCAAGAGTCTGTCTCTAGCCAA				
GAPDH	Sense	GCTTCACCACCTTCTTGATGTC	23	23	23	58 °C
	Antisense	GAGTATGTCGTGGAGTCTACTG				

of cytotrophoblasts were observed (fig. 1B). In the fetuses, increased apoptosis of hematopoietic cells was observed in the liver (fig. 1C). These observed changes were the same as those of our previous report (Sehata et al. 2003). TUNEL staining and morphometry examination demonstrated that apoptosis was significantly induced in the liver, placenta, and fetal liver by T-2 toxin treatment (figs. 1D, E, F and fig. 2).

Microarray analysis

The selected results of microarray analysis in the liver, placenta, and fetal liver from pregnant rats treated with T-2 toxin are shown in tables 2, 3 and 4. Tables show the selected genes that we mainly focused on (apoptosis, metabolizing enzyme genes, and oxidative stress-related genes). In the liver, the expression of 235 genes was induced and the 382 genes were suppressed by T-2 toxin. The expression of p53, p21, cyclin G, cyclin D3, Bax-α, BOD-L and extracellular signal-related kinase (ERK3) (cell cycle- and apoptosis-related genes) was increased. In addition, the expression of Thioredoxin reductase and heme oxygenase (oxidative stress-related genes) was also increased. On the other hand, the expression of lipid metabolism-related genes and drug metabolizing enzymes-related genes was suppressed. Gene expression of DNA polymerase alpha was also suppressed. The expression of liver catalase, thioredoxin and CuZnSOD genes was decreased (table 2).

In the placenta, the expression of 187 genes was increased and the expression of 181 genes was suppressed by T-2 toxin. Gene expression of c-fos, c-jun, gas-5, GADD45, and PCNA (cell cycle- and apoptosis-related

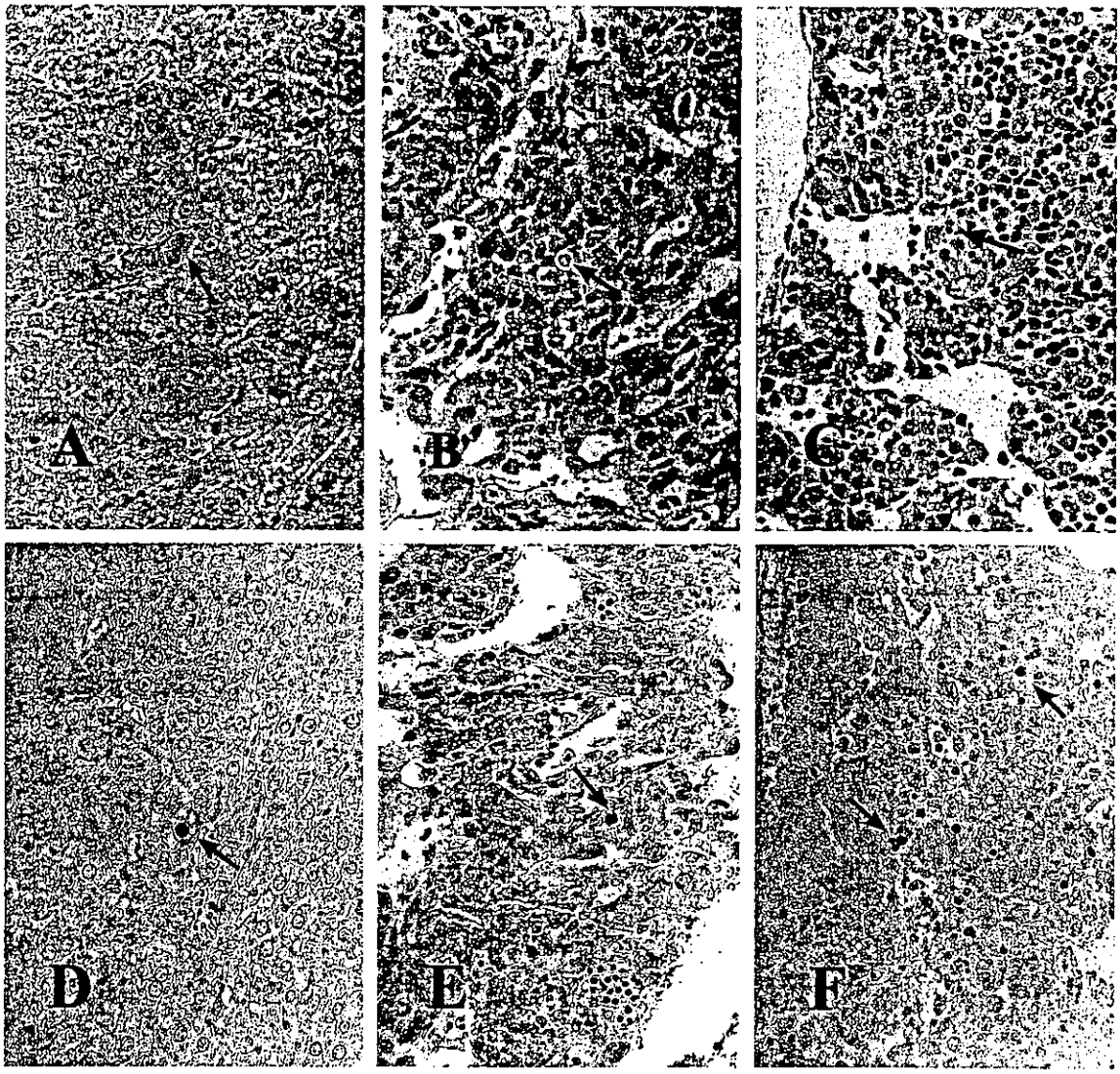

Fig. 1. Histopathological photographs of the liver, placenta and fetal liver from dams treated with T-2 toxin. Apoptotic cells (arrows) are detected in the liver (**A** and **D**), placenta (**B** and **E**) and fetal liver (**C** and **F**). HE staining, ×200 (A, B and C). TUNEL staining, ×200 (D, E and F).

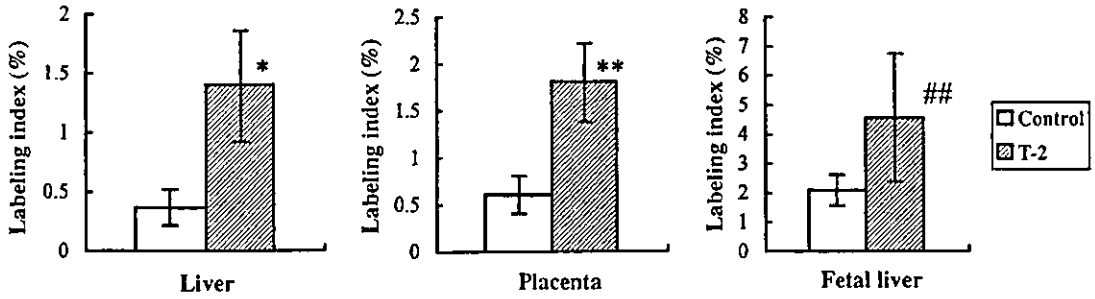

Fig. 2. TUNEL labeling index in the liver, placenta and fetal liver. Apoptosis was significantly induced by T-2 toxin in these tissues. Each value represents mean ± SD of 3 (liver) or 3/dam (placenta and fetal liver). * $p < 0.05$, ** $p < 0.01$ (Student's *t*-test), ## $p < 0.01$ (Welch's *t*-test): significantly difference from the control group.

Table 2. Gene expression changes in the dam liver treated with T-2 toxin.

Genes	Fold change	Accession No.
Apoptosis and cell cycle-related genes		
cyclin G	9.29##	X70871
p21 protein (cipl)	13.08**	L41275
extracellular signal-related kinase (ERK3)	3.29**	M64301
cyclin D3	1.66**	D16309
Bax-alpha	2.87#	U59184
nuclear oncoprotein p53	3.38**	X13058
14-3-3 protein mRNA for MSF S1 subunit	2.53**	D30740
Bcl-2 related ovarian death gene product BOD-L	1.89*	AF065433
gas-5 growth arrest homolog non-translated mRNA sequence	4.74#	U77829
DNA polymerase alpha	–8.79**	M15114
Lipid metabolism-related genes		
phospholipase A-2-activating protein (palp)	1.69**	U17901
PS-PLA1	8.92#	D88666
3-hydroxy-3-methylglutaryl coenzyme A reductase	5.37#	M29249
fatty acid translocase/CD36	–10.19**	AF072411
peroxisomal enoyl-CoA- hydrotase-3-hydroxyacyl-CoA bifunctional enzyme	–34.63**	K03249
isovaleryl-CoA dehydrogenase (IVD)	–4.58**	J05031
type I 5 alpha-reductase	–5.47##	S81448
very-long-chain acyl-CoA synthetase	–4.62**	D85100
Drug metabolizing enzyme genes		
glutathione S-transferase Yc1 subunit	–3.59**	S72505
CYP3A1	–6.62**	X64401
cytochrome P-450 ISF/BNF-G	–18.96##	M26127
cytochrome P450IIE1	–3.64**	M20131
liver glutathione S-transferase Ya subunit	–3.97**	K00136
cytochrome P-452	–1.78*	X07259
cytochrome P-450b (phenobarbital-inducible)	–7.23*	M11251
Stress-related genes		
thioredoxin reductase	4.14**	U63923
heme oxygenase	30.38#	J02722
liver catalase	–6.33**	M11670
thioredoxin	–1.37**	U73525
Cu, Zn superoxide dismutase	–2.04*	M25157

Significant difference from control; *, $p < 0.05$; **, $p < 0.01$ (Student's t-test); #, $p < 0.05$; ##, $p < 0.01$ (Welch's t-test).

genes) were induced. Gene expression of Nedd2/Ich-1 (Caspase-2) was also increased. Gene expression of Heat shock protein 70 was strongly increased by the treatment. On the other hand, the expression of lipid metabolism-related genes and glutathione S-transferase-related genes was suppressed by T-2 toxin. The expression of prolactin-like protein, spongiotrophoblast specific protein, cdk4 and DNA polymerase alpha was also suppressed (table 3).

In the fetal liver, the expression of 15 genes was increased and the expression of 103 genes was suppressed by T-2 toxin. The expression of heat shock protein 70 was strongly increased. The expression of Bax-α (apoptosis-related gene) was also increased. The expression of metabolism-related genes was generally not induced by T-2 toxin. On the other hand, the expression of lipid metabolism-related genes and glutathione S-transferases was suppressed. Gene expression of cyclin D, c-myc, cell cycle protein p55CDC and 14-3-3 protein was suppressed (table 4).

In comparison with the results of 3 tissues (liver, placenta, and fetal liver), changes in lipid metabolism-, apoptosis- and cell cycle-, and oxidative stress-related genes were detected in all tissues. Namely, decreased expression of lipid metabolism-related genes, increased expression of apoptosis- and cell cycle-related genes, and increased expression of oxidative stress-related genes were detected.

Semiquantitative RT-PCR

We performed semiquantitative RT-PCR on selected genes that we speculated the genes involved in the T-2 toxin-induced toxicity. table 5 and figure 3 show the results of RT-PCR analysis of drug metabolizing enzyme-related genes, apoptosis-related genes and oxidative stress-related genes. The gene expression of P450 isoenzymes and GSTs was suppressed by T-2 toxin in the liver. It showed the tendency of suppression in the placenta and fetal liver. Increased expression of apoptosis-related genes, p21 and c-jun, and p53 and Bax genes showed the tendency of suppression in the liver. In the placenta, increased expression of c-jun and GADD45 was detected, but there was no clear change in the fetal liver. Regarding the oxidative stress-related genes, the expression of heme oxygenase-1 in the liver, heat shock protein 70 in the placenta, and heme oxygenase-1 and heat shock protein 70 in the fetal liver was increased by

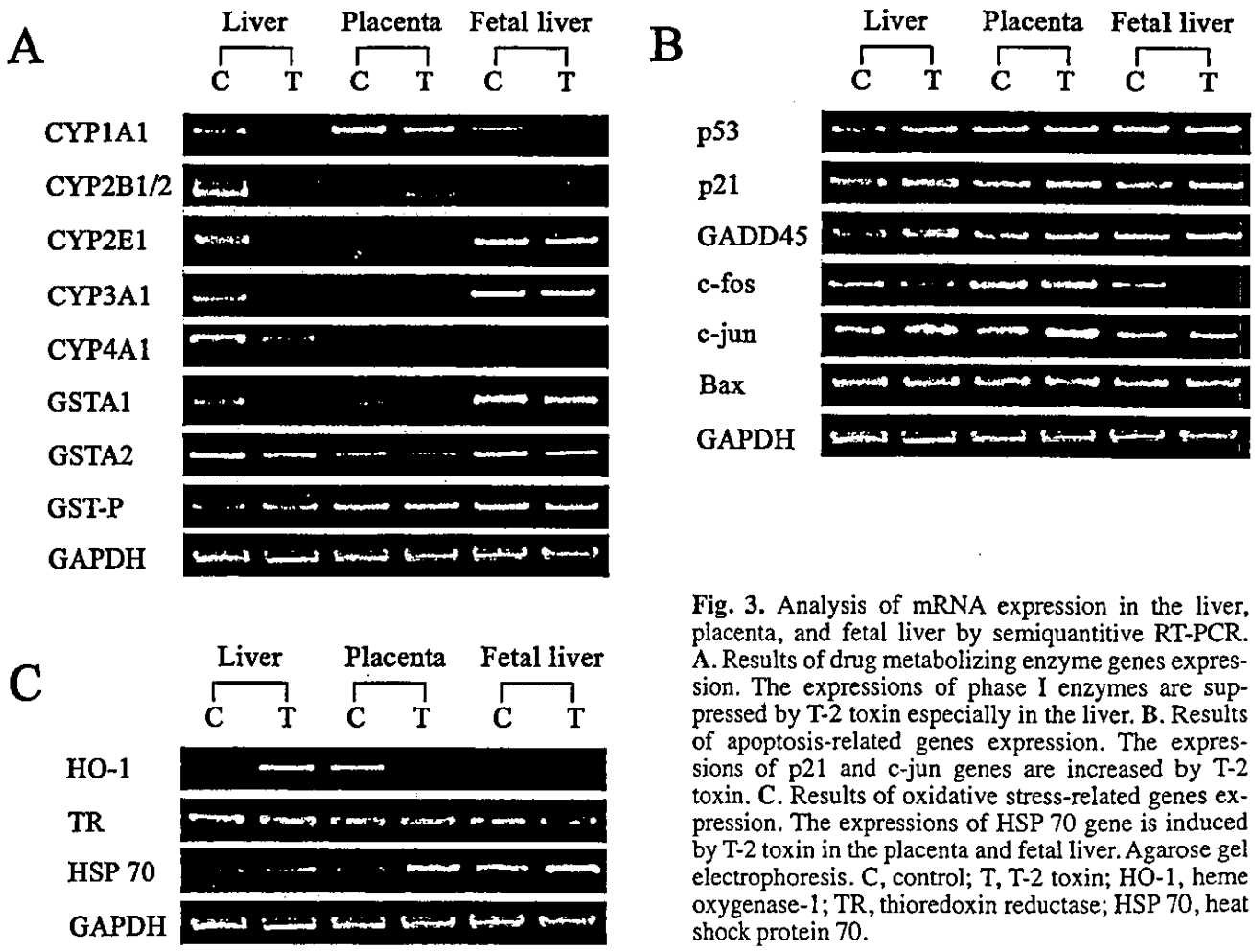

Fig. 3. Analysis of mRNA expression in the liver, placenta, and fetal liver by semiquantitive RT-PCR. A. Results of drug metabolizing enzyme genes expression. The expressions of phase I enzymes are suppressed by T-2 toxin especially in the liver. B. Results of apoptosis-related genes expression. The expressions of p21 and c-jun genes are increased by T-2 toxin. C. Results of oxidative stress-related genes expression. The expressions of HSP 70 gene is induced by T-2 toxin in the placenta and fetal liver. Agarose gel electrophoresis. C, control; T, T-2 toxin; HO-1, heme oxygenase-1; TR, thioredoxin reductase; HSP 70, heat shock protein 70.

Table 3. Genes expression changes in the placenta treated with T-2 toxin.

Genes	Fold change	Accession No.
Apoptosis and cell cycle-related genes		
c-fos	2.35**	X06769
c-jun oncogene mRNA for transcription factor AP-1	2.52**	X17163
gas-5 growth arrest homolog non-translated mRNA sequence	1.82**	U77829
GADD45	2.04**	L32591
Nedd2/Ich-1	1.44*	U77933
proliferating cell nuclear antigen (PCNA/cyclin)	1.85*	M24604
prolactin-like protein B	-2.24**	M31155
spongiotrophoblast specific protein	-6.11**	AB009890
cyclin-dependent kinase 4 (cdk4)	-1.49#	L11007
DNA polymerase alpha	-2.62**	M15114
Lipid metabolism-related genes		
phospholipase A-2-activating protein (palp)	1.53*	U17901
UCP2	2.04*	AB010743
thioesterase II	1.32*	Y00311
cytosolic 3-hydroxy 3-methylglutaryl coenzyme A synthase	-2.61**	X52625
acyl-coA oxidase	-1.58##	J02752
squalene epoxidase	-2.81**	D37920
hepatic squalene synthetase	-1.52**	M95591
stearoyl-CoA desaturase 2	-4.11**	AF036761
Drug metabolizing enzyme genes		
glutathione S-transferase (GST) Y(b) subunit	-1.63*	X04229
glutathione S-transferase P subunit	-1.63*	X02904
Stress-related genes		
hsp70.2 (heat shock protein 70)	9.67**	Z75029
heat shock protein (Hsp27)	1.31**	M86389
thioredoxin reductase	1.45**	U63923

Significant difference from control; *, $p < 0.05$; **, $p < 0.01$ (Student's t-test); #, $p < 0.05$; ##, $p < 0.01$ (Welch's t-test).

Table 4. Gene expression changes in the fetal liver treated with T-2 toxin.

Genes	Fold change	Accession No.
Apoptosis and cell cycle-related genes		
Bax-alpha	1.74**	U59184
cyclin D1	-1.67**	X75207
c-myc oncogene and flanking regions	-1.73#	Y00396
DNA polymerase alpha	-2.56**	M15114
cell cycle protein p55CDC	-2.09**	AF052695
14-3-3 protein beta subtype	-1.51#	S55223
Lipid metabolism-related genes		
squalene epoxidase	-3.89#	D37920
cytosolic 3-hydroxy 3-methylglutaryl coenzyme A synthase	-4.41**	X52625
farnesyl diphosphate synthase	-3.88**	M89945
2,3-oxidosqualene:lanosterol cyclase	-2.47#	D45252
fatty acid transporter	-4.11**	AB005743
Drug metabolizing enzyme genes		
glutathione S-transferase Yc2 subunit	-2.99#	S72506
glutathione S-transferase Yc1 subunit	-2.88*	S72505
Stress-related genes		
hsp70.2 (heat shock protein 70)	1039.12#	Z75029

Significant difference from control; *, $p < 0.05$; **, $p < 0.01$ (Student's t-test); #, $p < 0.05$ (Welch's t-test).

Table 5. Analysis of mRNA expression by semiquantitive RT-PCR.

Gene	Organs		
	Liver T-2 toxin	Placenta T-2 toxin	Fetal liver T-2 toxin
Drug-metabolizing enzyme genes			
CYP1A1	0.390 ± 0.639[a)]	0.706 ± 0.519	0.425 ± 0.374*
CYP2B1/2	0.107 ± 0.108**	1.105 ± 0.397	1.833 ± 1.318
CYP2E1	0.262 ± 0.130**	0.550 ± 0.492	0.937 ± 0.318
CYP3A1	0.281 ± 0.086**	1.828 ± 0.632	0.637 ± 0.499
CYP4A1	0.384 ± 0.203**	0.923 ± 0.166	0.646 ± 0.168*
GSTA1	0.324 ± 0.203*	0.516 ± 0.299*	0.682 ± 0.457
GATA2	0.529 ± 0.205#	0.687 ± 0.601	0.693 ± 0.467
GST-P	1.764 ± 1.071	0.873 ± 0.252	0.786 ± 0.480
Apoptosis-related genes			
p53	1.178 ± 0.297	1.215 ± 0.082	0.861 ± 0.232
p21	1.609 ± 0.382*	0.975 ± 0.196	1.061 ± 0.186
GADD45	1.469 ± 0.566	1.081 ± 0.043*	1.162 ± 0.212
c-fos	0.591 ± 0.226*	0.940 ± 0.067	0.540 ± 0.268
c-jun	1.809 ± 0.526*	1.271 ± 0.176*	0.915 ± 0.170
Bax	1.158 ± 0.156	0.928 ± 0.095	0.792 ± 0.150
Oxidative stress-related genes			
Heme oxygenase-1	5.290 ± 2.909*	0.353 ± 0.139	0.005 ± 0.004#
Thioredoxin reductase	1.198 ± 0.182	0.961 ± 0.025	0.937 ± 0.272
Heat shock protein 70	0.905 ± 0.303	3.291 ± 0.270**	2.093 ± 0.692*

Note. [a)], Relative band density. Mean ± SD.
Significant difference from control: *, $p < 0.05$; **, $p < 0.01$ (Student's t-test); #, $p < 0.05$ (Welch's t-test).

T-2 toxin. These results corresponded to the results from microarray analysis, although some genes showed opposite results from those of microarray analysis.

Discussion

It is reported that T-2 toxin induces apoptosis in the lymphoid tissues and intestine (Bratich et al. 1990; Hayes et al. 1982; Hoerr et al. 1981; Kosuri et al. 1971; Marasas et al. 1969; Pang et al. 1987). In the present study, the induction of apoptosis in the liver, placenta and fetal liver from pregnant rats treated with T-2 toxin was also observed. Apoptotic changes were also observed in the lymphoid tissues including the thymus and spleen, intestine, and fetal brain (Sehata et al. 2003). Therefore, T-2 toxin may induce the changes of the same nature in the liver, placenta, and fetal tissues. To examine the mechanism of T-2 toxin-induced toxicity in pregnant rats, Wistar rats on GD13 were treated orally with a single dose of T-2 toxin (2 mg/kg), and were sacrificed at 24 HAT, and Microarray analysis was performed in the liver, placenta and fetal liver.

From the results of microarray analysis, the expression of apoptosis/cell cycle-related genes, lipid metabolism-related genes, drug metabolizing enzyme genes and oxidative stress-related genes was detected in the liver, placenta and fetal liver. T-2 toxin enhances lipid peroxidation in the liver (Chang et al. 1988). Oxidative stress causes lipid peroxidation and induces mitochondrial dysfunction. This mitochondrial dysfunction causes fatty acid β-oxidation and induces fatty liver (Jaeschke et al. 2002). In the present study, fatty liver was observed in the liver, suggesting that the fatty change in the liver may be related with oxidative stress caused by T-2 toxin.

Increased apoptosis in the liver, placenta and fetal liver was observed histopathologically in the present study, and microarray analysis also showed the increased expression of apoptosis-related genes, p53, p21, Bax-α and BOD-L. At the same time, the expression of cell cycle accelerating genes, cyclin G and cyclin D3, was also induced by T-2 toxin. Furthermore, the expression of heat shock protein (HSP) 70 and HSP 27, oxidative stress-related genes and repressor of apoptosis (Garrido et al. 2001), was induced in the placenta and fetal liver. This suggests that T-2 toxin induced not only apoptosis but also cell repair and proliferation at 24 HAT.

It is reported that the gene expression of phase I and II enzymes was decreased by T-2 toxin (Galtier et al. 1989; Guerre et al. 2000). One of the causes is considered that T-2 toxin inhibits protein and DNA synthesis (Rosentein and Lafarge-Frayssinet 1983; Thompson and Wannemacher 1990). In the present study, the expression of P450 and GSTs genes in the liver was suppressed

by T-2 toxin. However, the expression of DNA synthesis-related genes was induced by T-2 toxin, suggesting that there are other mechanisms of P450 and GST suppression. As described above, T-2 toxin enhanced lipid peroxidation indicated by increased diene formation (CHANG et al. 1988). In addition, lipid peroxidation caused by oxidative stress might affect the P450 content in the liver (SERBINOVA et al. 1989). Therefore, oxidative stress might be an effective factor of P450 suppression. In the placenta and fetal liver, GST genes were suppressed by T-2 toxin in microarray analysis, and the results of RT-PCR also showed the tendency of suppression in these genes. In general, CYP3A1 expression was detected in the rat placenta and fetal liver through pregnancy (EJIRI et al. 2001; EJIRI et al. 2003). It is reported that CYP2B1, 2B2, 2E1 and 4A1 mRNAs were detected in the fetal liver, but other P450s were not done (BORLAKOGLU et al. 1993; OMIECINSKI et al. 1990). In the present study, although we detected all P450 genes examined, the expression differed by each gene. Moreover, these genes in the placenta and fetal liver showed the tendency of suppression by T-2 toxin treatment. The results obtained from RT-PCR were consistent with the results from the microarray analysis.

In comparison with the results from RT-PCR analysis on dam's liver and fetus, the expression levels of some genes showed opposite direction. The reason for these results is unclear, but it may suggest that there are differences in reaction to T-2 toxin and/or in responding genes to T-2 toxin between dam and fetus.

In the present study, rats on day 13 of gestation were treated orally with T-2 toxin and were sacrificed at 24 hours after treatment. Microarray analysis in the liver, placenta and fetal liver showed the same changes in lipid metabolism-related genes, drug metabolizing enzyme genes, apoptosis-related genes and oxidative stress-related genes. From these results, the mechanism of T-2 toxin-induced toxicity is speculated that T-2 toxin causes oxidative stress, following the impairment of lipid peroxidation and metabolism-related enzymes. These changes may cause the changes in the intracellular environments, finally resulting in the induction of apoptosis. Further study on the gene expression profiles at the earlier time point should be done to clarify the whole mechanisms of T-2 toxin-induced toxicity.

References

ALBARENQUE SM, SUZUKI K, SHINOZUKA J, et al.: Kinetics of apoptosis-related genes mRNA expression in the dorsal skin of hypotrichotic WBN/ILA-*Ht* rats after topical application of T-2 toxin. Exp Toxic Pathol 2001; **52**: 553–556.

BORLAKOGLU JT, SCOTT A, HENDERSON CJ, et al.: Expression of P450 isoenzymes during rat liver organogenesis. Int J Biochem 1993; **25**: 1659–1668.

BRATICH PM, BUCK WB, HASCHEK WM: Prevention of T-2 toxin-induced morphological effects in the rat by highly activated charcoal. Arch Toxicol 1990; **64**: 251–253.

BULERA SJ, EDDY SM, FERGUSON E, et al.: RNA expression in the early characterization of hepatotoxicants in Wistar rats by high-density DNA microarrays. Hepatology 2001; **33**: 1239–1258.

CHANG I-M and MAR W-C: Effect of T-2 toxin on lipid peroxidation in rats: elevation of conjugated diene formation. Toxicol Lett 1988; **40**: 275–280.

EJIRI N, KATAYAMA K, NAKAYAMA H, et al.: Expression of cytochrome P450 (CYP) isozymes in rat placenta through pregnancy. Exp Toxic Pathol 2001: **53**: 387–391.

EJIRI N, KATAYAMA K, Doi K: Induction of CYP3A1 by dexamethasone and pregnenolone-16_-carbonitrile in pregnant rat and fetal livers and placenta. Exp Toxic Pathol 2003: **54**: 273–279.

GALTIER P, PAULIN F, EECKHOUTTE C, et al.: Comparative effects of T-2 toxin and diacetoxyscirpenol on drug metabolizing enzymes in rat tissues. Food Chem Toxicol 1989; **27**: 215–220.

GAN L, LIU Q, XU H-B, et al.: Effects of selenium overexposure on glutathione peroxidase and thioredoxin reductase gene expressions and activities. Biol Trace Elem Res 2002; **89**: 165–175.

GARRIDO C, GURBUXANI S, RAVAGNAN L, et al.: Heat shock proteins: endogenous modulators of apoptotic cell death. Biochem Biophys Res Commun.2001; **286**: 433–442.

GOLUB TR, SLONIM DK, TAMAYO P, et al.: Molecular classification of cancer: class discovery and class prediction by gene expression monitoring. Science 1999; **286**: 531–537.

GUERRE P, EECKHOUTTE C, BURGAT V, et al.: The effects of T-2 toxin exposure on liver drug metabolizing enzymes in rabbit. Food Addit Contam 2000; **17**: 1019–1026.

HAYES MA and SCHIFFER FB: Comparative toxicity of dietary T-2 toxin in rats and mice. J Appl Toxicol 1982; **2**: 207–211.

HOERR FJ, CARLTON WW, YAGEN B: Mycotoxicosis caused by a single dose of T-2 toxin or diacetoxyscirpenol in broiler chickens. Vet Pathol 1981; **18**: 652–664.

IARC (INTERNATIONAL AGENCY FOR RESEARCH ON CANCER): (1993). Toxins derived from Fusarium sporotrichioides: T-2 toxin. In IARC monographs on the evaluation of carcinogenic risks to humans, Vol. 56, pp. 467–488. IARC (WHO Secretariat), Lyon.

ISHIGAMI N, SHINOZUKA J, KATAYAMA K, et al.: Apoptosis in mouse fetuses from dams exposed to T-2 toxin at different days of gestation. Exp Toxic Pathol 2001; **52**: 493–501.

JAESCHKE H, GORES GJ, CEDERBAUM A, et al.: Mechanisms of hepatotoxicity. Toxicol Sci 2002; **65**: 166–176.

KATAYAMA K, OHTSUKA R, TAKAI H, et al.: Expression of p53 and its transcriptional target genes mRNAs in the ethylnitrosourea-induced apoptosis and cell cycle arrest in the fetal central nervous system. Histol Histopathol 2002; **17**: 715–720.

KOSURI NR, SMALLEY EB, NICHOLS RE: Toxicologic studies of *Fusarium tricinctum* (corda) Synder et Hansen from moldy corn. Am J Vet Res 1971; **32**: 1843–1850.

LAFARGE-FRAYSSINET C, CHAKOR K, LAFONT P, et al.: Transplacentral transfer of T2-toxin: pathological effect. J Environ Pathol Toxicol Oncol 1990; **10**: 64–68.

LIU H, SONG D, LEE SS: Role of heme oxygenase-carbon monoxide pathway in pathogenesis of cirrhotic cardiomyopathy in the rat. Am J Physiol Gastrointest Liver Physiol 2001; **280**: G68–G74.

LUCERI C, CADERNI G, SANNA A, et al.: Red wine and black tea polyphenols modulate the expression of cycloxygenase-2, inducible nitric oxide synthase and glutathione-related enzymes in azoxymethane-induced F344 rat colon tumors. J Nutr 2002; **132**: 1376–1379.

LUEHE A, HILDEBRAND H, BACH U, et al.: A new approach to study ochratoxin A (OTA) induced nephrotoxicity: expression profiling in vivo and in vitro employing cDNA-microarrays. Toxicol Sci 2003; **73**: 315–328.

MARASAS WFO, BAMBURG JR, SMALLEY EB, et al.: Toxic effects on trout, rats and mice of T-2 toxin produced by the fungus *Fusarium tricinctum* (corda) Synder et Hansen. Toxicol Appl Pharmacol 1969; **15**: 471–482.

MORRIS DL and DAVILA JC: Analysis of rat cytochrome P450 isoenzyme expression using semi-quantitative reverse transcriptase-polymerase chain reaction (RT-PCR). Biochem Pharmacol 1996; **52**: 781–792.

NAKAHARA T, HIRANO M, UCHIYAMA H, et al.: Chronic alcohol feeding and its influence on c-fos and heat shock protein-70 gene expression in different brain regions of male and female rat. Metabolism 2002; **51**: 1562–1568.

OMIECINSKI CJ, HASSETT C, COSTA P: Developmental expression and *in situ* localization of the phenobarbital-inducible rat hepatic mRNAs for cytochromes CYP2B1, CYP2B2, CYP2C6, and CYP3A1. Mol Pharmacol 19990; **38**: 462–470.

PANG VF, LORENZANA RM, BEASLEY VR, et al.: Experimental T-2 toxicosis in swine: III. Morphologic changes following intravascular administration of T-2 toxin. Fundam Appl Toxicol 1987; **8**: 298–309.

ROSENTEIN Y and LAFARGE-FRAYSSINET C: Inhibitory effect of Fusarium T2-toxin on lymphoid DNA and protein synthesis. Toxicol Appl Pharmacol 1983; **70**: 283–288.

ROUSSEAUX CG AND SCHIEFER HB: Maternal toxicity, embryolethality and abnormal fetal development in CD-1 mice following one oral dose of T-2 toxin. J Appl Toxicol 1987; **7**: 281–288.

SEHATA S, TERANSHIM, ATSUMI F, et al.: T-2 toxin-induced morphological changes in pregnant rats. J Toxicol Pathol 2003; **16**: 59–65.

SERBINOVA EA, KAHIISKA MB, BAKALOVA RA, et al.: Lipid peroxidation activation and cytochrome P-450 decrease in rat liver endoplasmic reticulum under oxidative stress. Toxicol Lett 1989; **47**: 119–123.

STANFORD GK, HOOD RD, HAYES AW: Effect of prenatal administration of T-2 toxin to mice. Res Comm Chem Pathol Pharmacol 1975; **10**: 743–746.

THOMPSON WL and WANNEMACHER RW JR: In vivo effects of T-2 mycotoxin on synthesis of proteins and DNA in rat tissues. Toxicol Appl Pharmacol 1990: **105**: 483–491.

UENO M, KATAYAMA K, NAKAYAMA H, et al.: Mechanisms of 5-azacytidine (5AzC)-induced toxicity in the rat foetal brain. Int J Exp Path 2002; **83**: 139–150.

VANHASECKE T, LINDORS KO, OINONEN T, et al.: Effect of long-term ethanol exposure on the acinar distribution of hepatic glutathione S-transferase. Drug Metab Disposit 2000; **28**: 1470–1474.

WARINGJF, JOLLY RA, CIURLIONIS R, et al.: Clustering of hepatotoxins based on mechanism of toxicity using gene expression profiles. Toxicol Appl Pharmacol 2001; **175**: 28–42.

WHO (WORD HEALTH ORGANIZATION): Selected mycotoxins: ochratoxins, trichothecenes, ergot. Environmental Health Criteria 1990; **105**, WHO, Geneva.

YANG MCK, RUAN QG, YANG JJ, et al.: A statistical method for flagging weak spots improves normalization and ratio estimates in microarrays. Physiol Genomics 2001; **7**: 45–53.

Available online at www.sciencedirect.com

SCIENCE DIRECT

Experimental and Molecular Pathology 77 (2004) 214–221

Experimental and Molecular Pathology

www.elsevier.com/locate/yexmp

MHC class II-related genes expression in porcine-serum-induced rat hepatic fibrosis☆

Yasuko Baba*, Kunio Doi

Department of Veterinary Pathology, Graduate School of Agricultural and Life Science, The University of Tokyo, Tokyo 113-8657, Japan

Received 2 August 2004
Available online 30 September 2004

Abstract

Genes, especially MHC class II-related genes, expression was examined in porcine-serum (PS)-induced hepatic fibrosis model. Brown–Norway (BN) and Wistar rats were injected intraperitoneally with 0.5 ml sterile porcine serum twice a week for 1, 2, 3, 4, and 8 weeks. Histopathologically, inflammation started at 2 weeks in BN and at 4 weeks in Wistar rats, and hepatic fibrosis developed at 4 weeks in BN rats and at 8 weeks in Wistar rats. Microarray analysis done at 2 and 4 weeks revealed that the expression of MHC class II-related genes and acute phase inflammation-related genes significantly increased at 2 weeks in BN and at 4 weeks in Wistar rats. On the other hand, the expression of some transcription-related genes was down-regulated in both strains. In BN rats, the results of semiquantitative RT-PCR analysis done on four MHC class II-related genes mRNAs corresponded well with those of microarray analysis. MHC class II is considered to be involved in the initiation of PS-induced hepatic fibrosis in rats.

Keywords: Hepatic fibrosis; Porcine serum; MHC class II; Microarray; RT-PCR

Introduction

Although hepatic fibrosis is one of the important disorders in humans, detailed fibrogenic process and mechanisms of hepatic fibrosis are not fully clarified. To elucidate these points, many animal models have been developed as follows: models induced by carbon tetrachloride (Akiyoshi and Terada, 1998; Armbrust et al., 1997), radiation (Geraci et al., 1992; Peng et al., 1994), diethyl nitrosamine (Steinhoff, 1975; Xu et al., 1994), D-galactosamine (Jonker et al., 1994; Yang et al., 2002), bile duct resection (Rioux et al., 1996; Sugihara et al., 1999), and porcine serum (PS) (Ballardini et al., 1988; Bhunchet and Fujieda, 1993; Bhunchet and Wake, 1992; Bhunchet et al., 1996; Kitamura et al., 1984; Nakano, 1986; Senoo and Wake, 1985; Shiga et al., 1997). Differing from many postnecrotic hepatic fibrosis models, PS-induced hepatic fibrosis in rats is characterized by accompanying little hepatocyte damage (Bhunchet and Fujieda, 1993; Bhunchet and Wake, 1992; Fujiwara et al., 1988; Ishida et al., 1991). In our previous report of PS-induced hepatic fibrosis in rats, inflammatory infiltration and hepatic fibrosis occurred earlier in Brown–Norway (BN) rats than in Wistar rats (Baba et al., 2004). The present study was carried out to examine gene expression profiles in the early phase of PS-induced hepatic fibrosis in order to find a clue to clarify the pathogenesis of hepatic fibrosis and the cause of rat strain differences. BN rats are well known to show high immunoreactivities (Haczku et al., 1995; Uyama et al., 1995), and Wistar rats are frequently used in toxicologic studies.

The protocol of this study was approved by the Animal Care and Use Committee of Graduate School of Agricultural and Life Sciences, the University of Tokyo.

☆ Gene expression in porcine-serum-induced rat hepatic fibrosis.

* Corresponding author. Department of Veterinary Pathology, Graduate School of Agricultural and Life Science, The University of Tokyo, 1-1-1, Yayoi, Bunkyo-ku, Tokyo 113-8657, Japan. Fax: +81 3 5841 8185.
E-mail address: aa27157@mail.ecc.u-tokyo.ac.jp (Y. Baba).

0014-4800/$ - see front matter © 2004 Elsevier Inc. All rights reserved.
doi:10.1016/j.yexmp.2004.08.001

Materials and methods

Animals

Thirty 5-week-old male rats each of BN/Crj (BN) (90 ± 10 g) and Crj:Wistar (Wistar) strains (140 ± 10 g) were purchased from Charles River Japan Co., Kanagawa. The animals were housed three per cage using an isolator caging system (Niki Shoji Co., Tokyo) under controlled conditions (temperature: 23 ± 2°C, relative humidity: 55 ± 5%, and 12-12-h–dark cycle) and fed commercial pellets (MF, Oriental Yeast Co., Tokyo) and water ad libitum. The animals were subjected to the experiment after 1-week acclimation.

Treatments

The rats of each strain were equally divided into two groups. The treatment group was intraperitoneally (ip) injected with 0.5 ml/head of sterile porcine serum (PS) (COSMO BIO Co., Ltd.) twice a week for up to 8 weeks. The vehicle group was treated with sterile physiological saline (S) in the same way and served as controls. At 1, 2, 3, 4, and 8 weeks, three rats of each group were killed by blood sampling from the abdominal aorta under ether anesthesia at 24 h after the last injection, respectively.

The rats were weighed at 1, 2, 3, 4, and 8 weeks. At necropsy, the liver of each rat was also weighed, and the ratio of liver weight to body weight (relative liver weight) (g%) was calculated.

Histopathology

The liver excluding the left lateral lobe was fixed in 10% neutral-buffered formalin. Four-micrometer paraffin sections were stained with hematoxylin and eosin (HE) or Masson's trichrome and subjected to histopathological examination.

RNA extraction and microarray analysis

Total RNA was extracted from the frozen left lateral hepatic lobe using the RNeasy Protect Mini Kit (QIAGEN Inc., CA, USA). Total RNA samples were used for microarray analysis (two samples per group at 2 and 4 weeks) and reverse transcriptase polymerase chain reaction (RT-PCR) (three samples per group at 1, 2, 3, 4, and 8 weeks).

cDNA was prepared from 5 μg of total RNA using the SuperScript Double Strand cDNA Synthesis Kit (Invitrogen, CA, USA). T7-(dT)24 primer (primer sequence: 5′GGCCAGTGAATTGTAATACGACTCACTATAGGGA-GGCGG-(T) 24-3′), was used for first strand cDNA synthesis (Amersham Biosciences, Japan). Then, biotinylated cRNA was synthesized using the Enzo Bioarray High Yield RNA Transcription Labeling Kit (Enzo Diagnosis Inc., USA).

After 20 μg biotin-labeled cRNA was fragmented, hybridization solution was prepared using GeneChip® Eukaryotic Hybridization Control Kit (Affymetrix, USA) and was hybridized to the Affymetrix Rat Genome RAE 230A oligonucleotide array for 45°C for 16 h in GeneChip® Hybridization Oven 640 (Affymetrix). The chips were washed and stained using the Fluidics Station (Affymetrix) and scanned with GeneArray® Scanner (Affymetrix).

Data analysis

The microarray imaging data were analyzed using the proprietary software (GeneChip Microarray Suite, v. 5.0, Affymetrix). In brief, total array normalization was performed in each experimental data (Yang et al., 2001). Following this, data were compared between the PS-treated and control groups and were expressed as a fold change (log 10 ratio). Finally, we selected genes that gave a distinction value of greater than +1.0 or less than −1.0 (10-fold threshold). In the present study, we only analyzed known genes.

Semiquantitative reverse transcriptase polymerase chain reaction (RT-PCR)

Based on the results of microarray analysis and the report describing an immunohistochemical finding suggesting a participation of MHC class II in thioacetamide-induced rat hepatic fibrosis (Ide et al., 2003), we performed RT-PCR focusing on cellular markers genes. Total RNA was prepared as described above. The first strand cDNA was synthesized using oligo $(dT)_{12-18}$ primer and Superscript II RNase H-Reverse transcriptase (Invitrogen). PCR was performed using oligonucleotide primers sets corresponding to the cDNA sequences: CD74 antigen (MHC class II invariant chain), MHC class II alpha chain, MHC class II antigen RT1.B-1 beta chain, MHC class II RT1.D beta chain, and glyceraldehydes-3-phosphate dehydrogenase (GAPDH) (Table 1). In brief, 100 μl reaction mixture containing 76.5 μl RNase-free water, 10 μl 10× PCR buffer (100 mM Tris–HCl buffer, 500 mM KCl, and 15 mM $MgCl_2$; Takara Shuzo Co., Ltd., Japan), 10 μl dNTP (Takara), 1 μl 50 pmol sense and 1 μl 50 pmol antisense primers, 1 μl cDNA sample, and 0.5 μl 250 units recombinant *Taq* DNA polymerase (Takara) was prepared. After preheating at 95°C for 5 min, PCR reaction (cycle number: Table 1) was performed using Takara PCR Thermal cycler SP (Takara) as follows: denaturation at 95°C for 1 min, annealing at 58°C for 1 min, and extension at 72°C for 1 min. The PCR products were electrophoresed in 2% agarose S (Nippon Gene Co., LTD., Japan) or 1× TBE buffer (89 mM Tris–aminomethane, 89 mM Boric acid, 10 mM EDTA). The gels were stained with ethidium bromide (Sigma-Aldrich Co., USA). Fluorescent bands were visualized using a UV-CCD video system (EpiLight $_{UVFA1100}$;

Table 1
Primer sequences and cycle numbers

Gene	Sense primer (5′-3′)	Antisense primer (5′-3′)	Cycle number
CD 74 antigen	TGAAGAATGTTACCAAGTATGG	TGGTCAATACTTTAGGTGGAG	27
MHC class II alpha chain	AACCCTCCTCCCAGAAACTA	AGAACCCCAGCCAGACATTA	26
RT1.B beta chain	CCGTCACAAGCGTCAGAAAG	TGGGGAGGGGGTAAAGGAGT	27
RT1.D beta chain	GCACAAAATAAGAAGATGAG	CAGCCACCAGGAGCACAGAT	26
GAPDH	GCTTCACCACCTTCTTGATGTC	GAGTATGTCGTGGAGTCTACTG	21

AISIN COSMOS, Tokyo, Japan) and were analyzed using an imaging analysis software, Quantity One (pdi, USA), on a computer (Power Macintosh 8100/100 $_{AV}$). Relative intensity of the band against GAPDH band was represented as the mean ± standard error (SE) of three rats. Statistical analysis was performed by Student's *t* test.

Results

Changes in body and relative liver weights

Changes in the body weight were similar between the PS-treated and control groups in rats of both strains. In BN rats, the relative liver weight of the PS-treated group was significantly higher than that of the control group at 2 and 3 weeks.

Histological findings

In the PS-treated group, inflammatory cells mainly composed of macrophages were slightly infiltrated around the portal area of the liver at 2 weeks, and they increased thereafter in BN rats. On the other hand, inflammatory infiltration started at 4 weeks in Wistar rats. At 4 weeks, hepatic fibrosis occurred in BN rats but not in Wistar rats. At 8 weeks, hepatic fibrosis with formation of many small-sized pseudolobules developed in rats of both strains (Fig. 1). The liver of the control groups of both strains showed no histopathological changes.

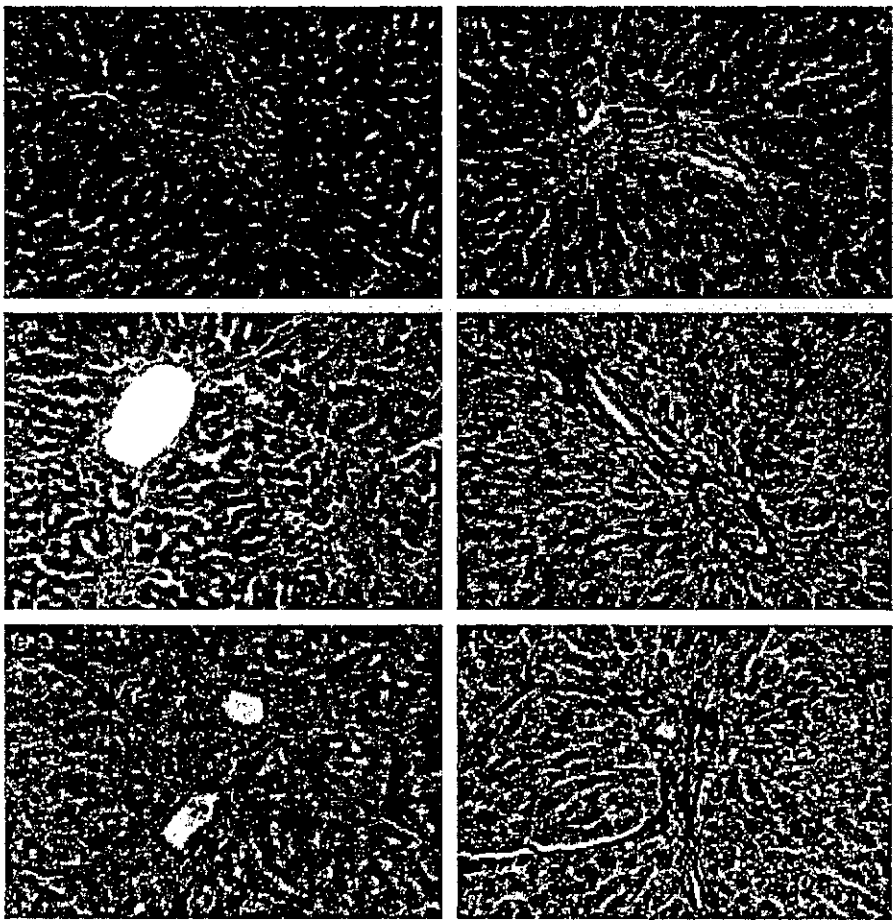

Fig. 1. Liver of BN (a, c, and e) and Wistar rats (b, d, and f) at 2 (a and b), 4 (c and d), and 8 weeks (e and f). Hepatic fibrosis is seen in BN rats but not in Wistar rats at 4 weeks. (a and b) HE ×151; (c–f) Masson's trichrome, ×151.